

1 Observation of radio galaxies with HAWC

Daniel Avila Rojas*, Rubén Alfaro

Instituto de Física, UNAM, Ciudad de México, México.

E-mail: daniel_avila5@ciencias.unam.mx, ruben@fisica.unam.mx

Antonio Galván, María Magdalena González, Nissim Fraija

Instituto de Astronomía, UNAM, Ciudad de México, México.

E-mail: agalvan@astro.unam.mx, magda@astro.unam.mx, nifraija@astro.unam.mx

Marc Klinger

Department of Physics, Aachen University, Germany.

E-mail: marc.klinger@rwth-aachen.de

for the HAWC Collaboration

For a complete author list, see <http://www.hawc-observatory.org/collaboration/>

The High Altitude Water Cherenkov (HAWC) Gamma-Ray Observatory is an extensive air shower array located in Puebla, Mexico. The closest radio galaxy within the HAWC field of view, M87, has been detected in very high energies. In this work we report upper limits on the TeV γ -ray flux of the radio galaxy M87. At a distance of 16 Mpc, M87 is a supergiant elliptical galaxy located in the Virgo Cluster that has been observed from radio wavelengths to TeV γ -rays. Although a single-zone synchrotron self-Compton model has been successfully used to explain the spectral energy distribution of this source up to a few GeV, the γ -ray spectrum at TeV has been interpreted within different theoretical models. We discuss the implications of these upper limits on the photo-hadronic interactions, as well as the number of neutrino events expected in the IceCube neutrino telescope.

35th International Cosmic Ray Conference – ICRC2017

10-20 July, 2017

Bexco, Busan, Korea

*Speaker.

2 1. Introduction

3 Active Galaxy nuclei (AGN) are one of the most powerful objects in the Universe. They
 4 are extraordinarily luminous across the entire electromagnetic spectrum, from radio to
 5 gamma rays. Radio galaxies, a type of AGN, are galaxies with non-thermal radio emission
 6 and lobes and jets emanating from the vicinity of the black hole. The spectral energy
 7 distribution (SED) is usually described by leptonic and hadronic models. Leptonic models
 8 can explain emission up to GeV energy range by means of synchrotron self-Compton (SSC)
 9 emission [1] and hadronic models at TeV energies by photo-hadronic processes [2, 3]. In
 10 accordance with the morphology, Fanaroff and Riley proposed two classifications [4]. Class
 11 I with the bright radio emission close to its center and Class II with the radio emission
 12 peak further away. The radio galaxy M87 being one the four radio galaxies observed in TeV
 13 γ -rays is of interest due to its closeness to the Earth affording us an excellent opportunity
 14 for detecting very-high-energy (VHE) photons. It is worth noting that this radio galaxy
 15 is the closest one in the field of view of the High Altitude Water Cherenkov (HAWC)
 16 Observatory. HAWC is continually monitoring M87 and although no detection has been
 17 detected yet, upper limits on its VHE flux have been obtained.

18 In this paper, upper limits on VHE flux are reported and a hadronic model is presented
 19 in order to constrain the amount of protons in the jet and then, the number of high-energy
 20 neutrinos that could be detected by IceCube. This work is arranged as follows. In Section
 21 2, we introduce the HAWC detector. In Section 3, we give a brief description of the radio
 22 galaxy M87. In Section 4 and 5 we show the data analysis and upper limits to the VHE
 23 flux, respectively. In Section 6 the proposed hadronic model and the neutrino expectation
 24 are displayed and finally, brief conclusions are given in Section 7.

25 2. The HAWC Observatory

26 The High Altitude Water Cherenkov Observatory is an array of 300 Water Cherenkov
 27 Detectors (WCDs) located in Sierra Negra, Mexico at an altitude of 4100 meter above sea
 28 level. It is designed to detect extensive air showers (EAS) produced in the atmosphere by
 29 VHE gamma-rays and/or cosmic rays via the Cherenkov light generated by the secondary
 30 charged particles passing through the WCDs. Each WCD has a 7.3m diameter tank with
 31 a 4.5m depth, and is filled with 200,000 liters of purified water. In addition, each tank is
 32 instrumented with 4 Photomultiplier Tubes (PMT), a 10-inch PMT located at its center,
 33 and other three 8-inch PMTs located around it. HAWC is sensitive to gamma rays with
 34 energies in the range from 1 to 100 TeV with a duty cycle $> 95\%$ and an instantaneous
 35 field of view of 2sr. This observatory has already detected gamma-ray fluxes from different
 36 sources [5] such as the Crab Nebula [6], Markarian 421 and Markarian 501 [7] among others.

37 3. M87

38 M87 located near the center of the Virgo cluster at a distance of 16.7 Mpc ($z = 0.0044$)
 39 [8] is classified as Fanaroff-Riley Class I (FRI) source. The supermassive black hole in its

40 nucleus has a mass of $M_{BH} \approx 3 - 6 \times 10^9 M_\odot$ [9]. It has a relativistic jet emerging from its
 41 nucleus that extends up to 2 kpc which has been studied in the X-rays by Chandra satellite
 42 [10]. VHE emission has been detected by different detectors such as MAGIC, HESS and
 43 VERITAS [11, 12]. In particular, VERITAS reported a photon index of $2.31 \pm 0.17_{stat} \pm$
 44 0.2_{sys} and a flux normalization of $7.4 \pm 1.3_{stat} \pm 1.5_{sys} \times 10^{-13} \text{cm}^{-2} \text{s}^{-1} \text{TeV}^{-1}$ [13].

45 4. Data Analysis

46 The likelihood method is used in order to estimate the significance of a source that has
 47 a low signal-to-noise ratio. The significance is directly related to the log-likelihood ratio by

$$TS = -2 \ln \left(\frac{\mathcal{L}_0}{\mathcal{L}} \right), \quad (4.1)$$

48 where TS is the test statistic, and \mathcal{L}_0 and \mathcal{L} are the likelihood of the Null (no source
 49 model) and the Alternative (source model) hypotheses, which are modeled as a Poisson
 50 distribution of the event counts in each analysis and spatial bin i . They can be written as

$$\mathcal{L}_0 = \prod_i \ln \left(\frac{(B_i)^{N_i} e^{-(B_i)}}{N_i!} \right), \quad (4.2)$$

51 and

$$\mathcal{L} = \prod_i \ln \left(\frac{(B_i + S_i)^{N_i} e^{-(B_i + S_i)}}{N_i!} \right), \quad (4.3)$$

52 where S_i is the sum of the expected number of signal counts corresponding to a source
 53 with an specific spectra, B_i is the number of background counts observed, and N_i is the
 54 total number of counts observed. Therefore, TS is given by

$$TS = \sum_i 2 \left[N_i \ln \left(1 + \frac{S_i}{B_i} \right) - S_i \right]. \quad (4.4)$$

55 To set a 95% Confidence Level (CL) limit on the flux expected from the source we
 56 found the value of S_i that maximizes the TS , $TS_{(max)}$, and then optimize $\Delta TS = TS_{(max)} -$
 57 $TS_{(95)}$, such that [14]

$$2.71 = TS_{(max)} - TS_{(95)} = TS_{(max)} - \sum_i 2 \left[N_i \ln \left(1 + \frac{\xi S_i^{(ref)}}{B_i} \right) - \xi S_i^{(ref)} \right]. \quad (4.5)$$

58 Here, the number of expected signal counts from a source is scaled by a scale factor
 59 ξ , $S_i^{(ref)}$ is the expected number of signal counts in a bin calculated for a reference source
 60 spectral model and the flux normalization is $\langle F_0 \rangle_{(ref)}$. The scale factor ξ is then used to
 61 set a 95% CL limit for a particular source

$$\langle F_0 \rangle_{(95)} = \xi \times \langle F_0 \rangle_{(ref)}. \quad (4.6)$$

62 The limit is independent of the value chosen for $\langle F_0 \rangle_{(ref)}$. The Likelihood method is
 63 implemented in the HAWC software utility LIFF [15].

64 **5. Upper Limits**

65 The relevance of the detection of VHE gamma-rays from this radio galaxy is that it
 66 could constrain the different models used to describe the particle accelerations in AGN as
 67 well as the region where this occurs. Within the AGN unification models it was thought
 68 that only blazars type were expected to be observed in the VHE emission band. The
 69 detection of variable VHE gamma-rays from M87 motivated the re-examination of the
 70 acceleration processes in non-aligned AGNs [16].

71 Since the HAWC Observatory has not detected M87 with a statistical significance
 72 above 5σ , upper limits for the flux normalization of a point like source were calculated
 73 for M87 using 760 days of data. It was also taken into consideration the effect of Ex-
 74 tragalactic Background Light (EBL), so that the upper limit was calculated under two
 75 assumptions: one without EBL attenuation, since M87 is a nearby galaxy this is not an
 76 unlikely scenario[17]; and the one which assumes the Franceschini EBL model [18].

77 Table 1 reports the flux normalization limit calculated with the likelihood method for
 78 M87. Figure 1 shows the comparison of the calculated upper limit with the observations
 79 of other experiments.

Radio Galaxy	Upper Limit [$10^{-13} \text{ TeV}^{-1} \text{ cm}^{-2} \text{ s}^{-1}$]	UL with EBL [$10^{-13} \text{ TeV}^{-1} \text{ cm}^{-2} \text{ s}^{-1}$]
M87	1.89	3.51

Table 1: Upper limits calculated for M87 with and without EBL.

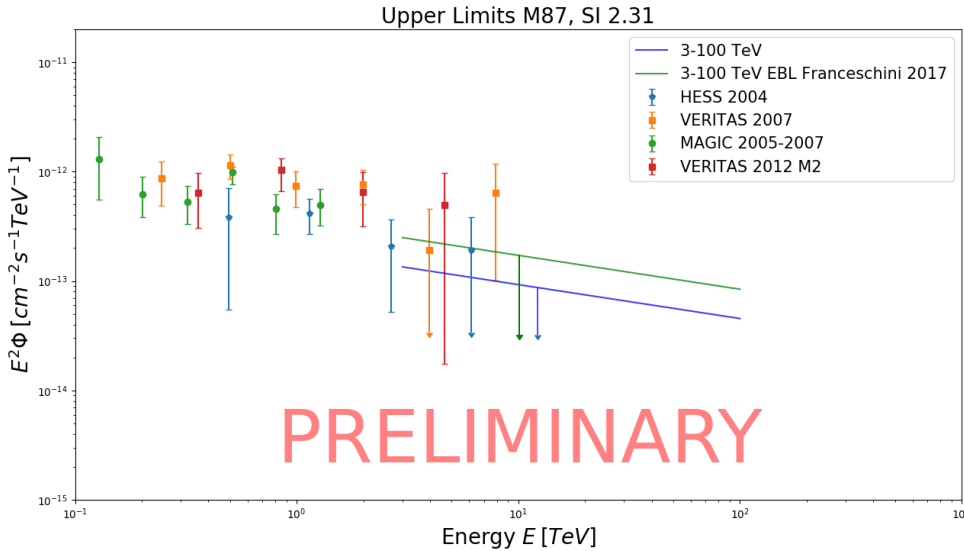


Figure 1: Upper limits calculated for M87. A comparison with the observations from MAGIC, HESS and VERITAS is shown.

80 The HAWC upper limit for M87 without accounting for the EBL is below the extrap-
 81 olation from the other experiments observations at energies beyond 1 TeV. This could

82 mean that M87 is in a very low state never detected before, or the existence of a cutoff
 83 on its spectrum. Results based on including the Franceschini EBL model are consistent
 84 with the observations but are not the more likely scenario because of the closeness and the
 85 strong EBL attenuation predicted by the Franceschini's model while observations of other
 86 AGNs may point to a weaker EBL attenuation [19]. The most recent observation by other
 87 experiments is the one made by VERITAS on 2012. All previous observations were made
 88 when M87 was in a low flux state. Because HAWC sees the average emission of the source,
 89 the upper limits account for possible flaring.

90 6. Hadronic Model

91 Radio Galaxies have been proposed as a powerful accelerator of cosmic rays. Acceler-
 92 ated protons can be described through a simple power law [20]

$$\left(\frac{dN}{dE}\right)_p = A_p E_p^{-\alpha_p}, \quad (6.1)$$

93 with A_p the proportionality constant and α_p the spectral power index. The proton density
 94 can be written as

$$U_p = \frac{L_p}{4\pi\delta_D^2 r_d^2}, \quad (6.2)$$

95 where r_d is the emitting region, δ_D is the Doppler factor and L_p is the proton luminosity
 96 which is given by

$$L_p = 4\pi d_z^2 A_p \int E_p E_p^{-\alpha_p} dE_p. \quad (6.3)$$

97 Accelerated protons loss their energies by electromagnetic channels and hadronic interac-
 98 tions. We consider that protons will be cooled down by $p\gamma$ interactions at the emitting
 99 region. Charged (π^+) and neutral (π^0) pions are obtained from $p\gamma$ interaction through the
 100 following channels

$$p\gamma \longrightarrow \Delta^+ \longrightarrow \begin{cases} p\pi^0 & \text{fraction } 2/3, \\ n\pi^+ & \text{fraction } 1/3, \end{cases} \quad (6.4)$$

101 After that a neutral pion decays into photons, $\pi^0 \rightarrow \gamma\gamma$, carrying 20% ($\xi_{\pi^0} = 0.2$) of the
 102 proton's energy, E_p . The efficiency of the photo-pion production is [21, 22]

$$f_{\pi^0} \simeq \frac{t_{\text{dyn}}}{t_{\pi^0}} = \frac{r_d}{2\gamma_p^2} \int d\epsilon \sigma_\pi(\epsilon) \xi_{\pi^0} \epsilon \int dx x^{-2} \frac{dn_\gamma}{d\epsilon_\gamma}(\epsilon_\gamma = x), \quad (6.5)$$

103 where t_{dyn} and t_{π^0} are the dynamical and the photo-pion timescales [22], respectively,
 104 $dn_\gamma/d\epsilon_\gamma$ is the spectrum of seed photons, $\sigma_\pi(\epsilon_\gamma)$ is the cross section of pion production
 105 and γ_p is the proton Lorentz factor. Taking into account that photons are released in the
 106 energy the range from ϵ_γ to $\epsilon_\gamma + d\epsilon_\gamma$ by protons in the energy range from E_p to $E_p + dE_p$,
 107 then $f_{\pi^0} E_p (dN/dE)_p dE_p = \epsilon_{\pi^0, \gamma} (dN/d\epsilon)_{\pi^0, \gamma} d\epsilon_{\pi^0, \gamma}$, then photo-pion spectrum is given by

$$\left[\epsilon_\gamma^2 \frac{dN_\gamma}{d\epsilon_\gamma}\right]_{\gamma, \pi^0} = A_{p\gamma} \begin{cases} \left(\frac{\epsilon_{\gamma, c}^{\pi^0}}{\epsilon_0}\right)^{-1} \left(\frac{\epsilon_\gamma}{\epsilon_0}\right)^{-\alpha_p+3} & \epsilon_\gamma < \epsilon_{\gamma, c}^{\pi^0} \\ \left(\frac{\epsilon_\gamma}{\epsilon_0}\right)^{-\alpha_p+2} & \epsilon_{\gamma, c}^{\pi^0} < \epsilon_\gamma, \end{cases} \quad (6.6)$$

108 where the proportionality constant $A_{p\gamma}$ is in the form

$$A_{p\gamma} = \frac{L_{\gamma,IC} \sigma_{\pi} \Delta\epsilon_{\text{res}} \epsilon_0^2 \left(\frac{2}{\xi_{\pi^0}}\right)^{1-\alpha_p}}{4\pi \delta_D^2 r_d \epsilon_{\text{pk,ic}} \epsilon_{\text{res}}} A_p, \quad (6.7)$$

109 $\epsilon_0 = 1$ TeV is the energy normalization, $\epsilon_{\text{pk,ic}}$ and $L_{\gamma,IC}$ are the energy and photon lumi-
 110 nosity of the second SSC peak, respectively, $\Delta\epsilon_{\text{res}} \approx 0.2$ GeV, $\epsilon_{\text{res}} \approx 0.3$ GeV and $\epsilon_{\gamma,c}^{\pi^0}$ is the
 111 break photon-pion energy given by $\epsilon_{\gamma,c}^{\pi^0} \simeq 31.87 \text{ GeV} \delta_D^2 \left(\frac{\epsilon_{\text{pk,ic}}}{\text{MeV}}\right)^{-1}$.

112

113 Taking into consideration the upper limit derived in the previous section and the
 114 values of Doppler factor, photon Luminosity of the second peak, emitting region and the
 115 power index of proton distribution, derived in [23], we found that the proton density and
 116 luminosity are less than 2.07 erg/cm^3 and $3.76 \times 10^{43} \text{ erg/s}$, respectively, when the EBL
 117 absorption is not considered and 3.83 erg/cm^3 and $6.96 \times 10^{43} \text{ erg/s}$ when we consider the
 118 EBL absorption.

119 6.1 High-energy neutrino expectation

120 Photo hadronic interactions in the emitting region also generate neutrinos through the
 121 charged pion decay products ($\pi^{\pm} \rightarrow \mu^{\pm} + \nu_{\mu}/\bar{\nu}_{\mu} \rightarrow e^{\pm} + \nu_{\mu}/\bar{\nu}_{\mu} + \bar{\nu}_{\mu}/\nu_{\mu} + \nu_e/\bar{\nu}_e$). Taking into
 122 account the distance of M87, the neutrino flux ratio (1 : 2 : 0) created on the source will
 123 arrive on the standard ratio (1 : 1 : 1) [24, 25]. The neutrino spectrum produced by the
 124 photo hadronic interactions is

$$\left[E_{\nu}^2 \frac{dN_{\nu}}{dE_{\nu}} \right] = A_{\nu} \epsilon_0^2 \begin{cases} \left(\frac{E_{\nu}}{\epsilon_0}\right)^2 & E_{\nu} < E_{\nu,c} \\ \left(\frac{E_{\nu}}{\epsilon_0}\right)^{2-\alpha_{\nu}} & E_{\nu,c} < E_{\nu} \end{cases} \quad (6.8)$$

125 where the factor A_{ν} normalized through the TeV γ -ray flux is $A_{\nu} = A_{p\gamma} \epsilon_0^{-2} 2^{-\alpha_p}$. The num-
 126 ber of neutrino events (N_{ev}) expected in a detector considering a neutrino flux dN_{ν}/dE_{ν}
 127 during a period T , can be derived through the following relation [23]

$$N_{\text{ev}} \simeq T \int_{E_{\nu}^{\text{th}}} A_{\text{eff}}(E_{\nu}) \frac{dN_{\nu}}{dE_{\nu}} dE_{\nu}, \quad (6.9)$$

128 where E_{ν}^{th} is the threshold energy and A_{eff} is the effective area¹ of the instrument.

129

130 Taking into consideration that a neutral pion decays into two photons and a charged
 131 pion into three (anti)neutrinos and a lepton, and also that the three neutrino flavors (ν_e , ν_{μ}
 132 and ν_{τ}) are presented, then $\left[E_{\nu}^2 \frac{dN_{\nu}}{dE_{\nu}} \right] \simeq \left[\epsilon_{\gamma}^2 \frac{dN_{\gamma}}{d\epsilon_{\gamma}} \right]_{\gamma,\pi^0}$. From eq. (6.9) and the effective area
 133 of the IceCube telescope for a point-like source in the declination of M87 [26], we found
 134 that the upper limit on the number of neutrinos detected would be (considering electron,
 135 muon and tau neutrinos) $\sim 10^{-2}$. It is worth noting that the upper limit derived is far
 136 below the IceCube sensitivity flux [26].

¹<https://icecube.wisc.edu/science/data>

137 7. Summary

138 The 95% CL upper limits on the flux normalization for the radio galaxy M87 were
 139 presented and discussed. The limits were calculated using 760 days of data collected
 140 with the HAWC Observatory. Within the proposed hadronic scenario we link the upper
 141 limits with the luminosity of accelerating protons in the jet. Considering the upper limits
 142 we constrain the amount of protons and then, the neutrino events expected in IceCube
 143 neutrino telescope. The HAWC observatory will continue monitoring M87 in order to
 144 detect very-high-energy photons in the following years.

145 8. Acknowledgments

146 We acknowledge the support from: the US National Science Foundation (NSF); the US
 147 Department of Energy Office of High-Energy Physics; the Laboratory Directed Research
 148 and Development (LDRD) program of Los Alamos National Laboratory; Consejo Nacional
 149 de Ciencia y Tecnología (CONACyT), México (grants 271051, 232656, 260378, 179588,
 150 239762, 254964, 271737, 258865, 243290, 132197), Laboratorio Nacional HAWC de rayos
 151 gamma; L'OREAL Fellowship for Women in Science 2014; Red HAWC, México; DGAPA-
 152 UNAM (grants RG100414, IN111315, IN111716-3, IA102715, 109916, IA102917); VIEP-
 153 BUAP; PIFI 2012, 2013, PROFOCIE 2014, 2015; the University of Wisconsin Alumni
 154 Research Foundation; the Institute of Geophysics, Planetary Physics, and Signatures at
 155 Los Alamos National Laboratory; Polish Science Centre grant DEC-2014/13/B/ST9/945;
 156 Coordinación de la Investigación Científica de la Universidad Michoacana. Thanks to
 157 Luciano Díaz and Eduardo Murrieta for technical support.

158 References

- 159 [1] Fraija, N., *Gamma-ray fluxes from the core emission of Centaurus A: a puzzle solved*,
 160 *MNRAS*, **441**:1209, 2014
- 161 [2] Petropoulou, M. and Lefa, E. and Dimitrakoudis, S. and Mastichiadis, A., *One-zone*
 162 *synchrotron self-Compton model for the core emission of Centaurus A revisited*, *AAP*,
 163 **562**:12, 2014
- 164 [3] Fraija, N., *Correlation of γ -Ray and High-energy Cosmic Ray Fluxes from the Giant Lobes of*
 165 *Centaurus A*, *ApJ*, **783**:44, 2014
- 166 [4] Fanaroff, B. L., Riley, J. M. *The Morphology of Extragalactic Radio Sources of High and Low*
 167 *Luminosity Mon. Not. R. Astron. Soc.*, **167**, 1974
- 168 [5] A.U. Abeysekara *et al.* (The HAWC Collaboration), *The 2HWC HAWC Observatory Gamma*
 169 *Ray Catalog*, [[astro-ph.HE/1702.02992v1](#)]
- 170 [6] A.U. Abeysekara *et al.* (The HAWC Collaboration), *Observation of the Crab Nebula with the*
 171 *HAWC Gamma-Ray Observatory*, [[astro-ph.HE/1701.01778v1](#)]
- 172 [7] A.U. Abeysekara *et al.* (The HAWC Collaboration), *Daily Monitoring of TeV Gamma-Ray*
 173 *Emission from Mrk 421, Mrk 501, and the Crab Nebula with HAWC*, *ApJ*, **841**:100 (13pp),
 174 2017 June 1

- 175 [8] S. Mei *et al.*, *The ACS Virgo Cluster Survey. XIII. SBF Distance Catalog and the*
176 *Three-dimensional Structure of the Virgo Cluster*, *ApJ*, **655**:144-162, January 2007
- 177 [9] J. L. Walsh, A. J. Barth, L. C. Ho and M. Sarzi *The M87 Black Hole Mass from*
178 *Gas-dynamical Models of Space Telescope Imaging Spectrograph Observations*, *Apj*, **770**:86
179 (11pp),2013 June Lfinal
- 180 [10] A. S. Wilson and Y. Yang, *Chandra X-Ray Imaging and Spectroscopy of the M87 Jet and*
181 *Nucleus*, *ApJ*, **568**:133-140, 2002 March
- 182 [11] J. Aleksić *et al.*, *MAGIC observations of the giant radio galaxy M 87 in a low-emission state*
183 *between 2005 and 2007*, *AAP*, **544**:A96, 2012 August
- 184 [12] M. Beilicke *et al.*, *Discovery of fast variability of the TeV γ -ray flux from the radio galaxy M*
185 *87 with H.E.S.S.*, *The 30th International Cosmic Ray Conference*, **ICRC 2008**, (Mérida,
186 México) p. 937
- 187 [13] V. A. Acciari *et al.* *Observation of Gamma-Ray Emission from the Galaxy M87 above 250*
188 *GeV with VERITAS*, *ApJ*, **679**:397-403, 2008 May
- 189 [14] A. Albert *et al.*, *Dark Matter Limits From Dwarf Spheroidal Galaxies with The HAWC*
190 *Gamma-Ray Observatory*, 2017 June [arXiv:1706.01277]
- 191 [15] P. W. Young, R. J. Lauer, G. Vianello, J. P. Harding, H. A. A. Solares, H. Zhou, M. Hui, for
192 the HAWC Collaboration, *A high-level analysis framework for HAWC*, *The 34th*
193 *International Cosmic Ray Conference*, **ICRC 2015**, edited by PoS (The Hague, The
194 Netherlands, 2015) p. 948
- 195 [16] F. M. Rieger and F. A. Aharonian, *Variable VHE gamma-ray emission from non-blazar*
196 *AGNs*, *A&A*, **479**:L5-L9 2008
- 197 [17] R. C. Gilmore *et al.*, *Semi-analytic modelling of the extragalactic background light and*
198 *consequences for extragalactic gamma-ray spectra*, *MNRAS* **422**:3189-3207, 2012 June
- 199 [18] A. Franceschini and G. Rodighiero, *The extragalactic background light revisited and the*
200 *cosmic photon-photon opacity*, 2017 May [arXiv:1705.10256]
- 201 [19] A. Domínguez *et al.*, *Detection of the Cosmic γ -Ray Horizon from Multiwavelength*
202 *Observations of Blazars*, *ApJ*,**770**:77, 2013 June
- 203 [20] Fraija, N. and González, M. M. and Perez, M. and Marinelli, A., *How Many Ultra-high*
204 *Energy Cosmic Rays Could we Expect from Centaurus A?*, *ApJ*, **753**:40F, 2012
- 205 [21] F. W. Stecker, *Effect of Photomeson Production by the Universal Radiation Field on*
206 *High-Energy Cosmic Rays*, *Physical Review Letters*, **21**:1016-1018, 1968 September
- 207 [22] E. Waxman and J. Bahcall, *High Energy Neutrinos from Cosmological Gamma-Ray Burst*
208 *Fireballs*, *Physical Review Letters*, **78**:2292-2295, 1997 March
- 209 [23] Fraija, N. and Marinelli, A., *Neutrino, γ -Ray, and Cosmic-Ray Fluxes from the Core of the*
210 *Closest Radio Galaxies*, *ApJ*, **830**:81, 2016
- 211 [24] Fraija, N., *GeV-PeV neutrino production and oscillation in hidden jets from gamma-ray*
212 *bursts*, *MNRAS*, **437**:2187, 2014
- 213 [25] Fraija, N., *Propagation and Neutrino Oscillations in the Base of a Highly Magnetized*
214 *Gamma-Ray Burst Fireball Flow*, *ApJ*, **787**:140, 2014
- 215 [26] Aartsen, M. G. and et al., *Searches for Extended and Point-like Neutrino Sources with Four*
216 *Years of IceCube Data*, *ApJ*, **796**:109, 2014